THE JOURNAL OF BIOLOGICAL CHEMISTRY VOL. 282, NO. 21, pp. 15559–15568, May 25, 2007

Flippase Activity Detected with Unlabeled Lipids by Shape Changes of Giant Unilamellar Vesicles*[S]

Received for publication, May 17, 2006, and in revised form, March 16, 2007 Published, JBC Papers in Press, March 17, 2007, DOI 10.1074/jbc.M604740200

Andreas Papadopulos[‡1], Stefanie Vehring[‡1,2], Iván López-Montero[§3], Lara Kutschenko[‡], Martin Stöckl[‡], Philippe F. Devaux[§3], Michael Kozlov[¶], Thomas Pomorski[‡4], and Andreas Herrmann[‡5]

From the [‡]Humboldt-Universität zu Berlin, Mathematisch-Naturwissenschaftliche Fakultät I, Institut für Biologie/Biophysik, Invalidenstrasse 42, D-10115 Berlin, Germany, [§]Institut de Biologie Physico-Chimique, 13 rue Pierre et Marie Curie, 75005 Paris, France, and [¶]Department of Physiology and Pharmacology, Sackler Faculty of Medicine, Tel Aviv University, 69978 Tel Aviv, Israel

Transbilayer movement of phospholipids in biological membranes is mediated by energy-dependent and energy-independent flippases. Available methods for detection of flippase mediated transversal flip-flop are essentially based on spin-labeled or fluorescent lipid analogues. Here we demonstrate that shape change of giant unilamellar vesicles (GUVs) can be used as a new tool to study the occurrence and time scale of flippase-mediated transbilayer movement of unlabeled phospholipids. Insertion of lipids into the external leaflet created an area difference between the two leaflets that caused the formation of a bud-like structure. Under conditions of negligible flip-flop, the bud was stable. Upon reconstitution of the energy-independent flippase activity of the yeast endoplasmic reticulum into GUVs, the initial bud formation was reversible, and the shapes were recovered. This can be ascribed to a rapid flip-flop leading to relaxation of the monolayer area difference. Theoretical analysis of kinetics of shape changes provides self-consistent determination of the flip-flop rate and further kinetic parameters. Based on that analysis, the half-time of phospholipid flip-flop in the presence of endoplasmic reticulum proteins was found to be on the order of few minutes. In contrast, GUVs reconstituted with influenza virus protein formed stable buds. The results argue for the presence of specific membrane proteins mediating rapid flip-flop.

In lipid bilayers the spontaneous movement of major phospholipids, *e.g.* of phosphatidylcholine (PC),[6] between the two monolayers is slow, with half-times on the order of hours or even days. However, lipid topology of cellular membranes results from a continuous bidirectional movement (flip-flop) of lipids between the two leaflets in which specific membrane proteins, so called flippases, play an essential role (1, 2). Energy-independent flippases allow phospholipids to equilibrate rapidly between the two monolayers, whereas energy-dependent flippases mediate a net transfer of specific phospholipids to one leaflet of the membrane. Candidates for the latter flippase are members of a conserved subfamily of P-type ATPases (2) as well as ATP binding cassette transporters (3).

In eukaryotes the cytoplasmic leaflet of the endoplasmic reticulum (ER) membrane is the major site of phospholipid biosynthesis. To ensure stable membrane growth, energy-independent flippases mediate rapid, bidirectional, and rather unspecific phospholipid flip-flop with half-times of minutes or less (4–7). A similar flippase activity was also found in the bacterial inner membrane, where lipid synthesis occurs likewise at the cytoplasmic leaflet (8).

Techniques to determine transbilayer phospholipid movement as well as the activity of flippases have been critically evaluated (9). Spin-labeled and fluorescent lipid analogues have provided much insight into protein-mediated transbilayer dynamics of phospholipids (9). However, the bulky reporter moieties may affect the absolute values of transbilayer lipid movement.

An alternative approach to characterize flip-flop is based on shape changes of deflated, prolate giant unilamellar vesicles (GUVs) (10), which do not require labeled lipid analogues. Shape transitions can be triggered by a very small excess of lipid in one monolayer (11–14). For example, unlabeled lipids were inserted into the external leaflet of GUVs made of egg-PC (11). Because of the low compressibility of lipid monolayers, the asymmetric lipid supply creates a surface area difference between the two leaflets, which in turn results in formation of a bud-like structure (Fig. 1*A*). If lipids (*e.g.* lyso-PC, LPC) that are known to undergo a very slow flip-flop similar to that of egg-PC were added, the bud was stable, whereas if the added lipids (*e.g.* ceramide) were able to rapidly redistribute between the two membrane leaflets, the initial bud formation was reversible, and the prolate shape was recovered (11). This can be explained by a relaxation of the monolayer area difference due to the trans-

* This work was supported in part by Deutsche Forschungsgemeinschaft Grant He1928–6 (to A. H.) and Po748–4 (to T. P.). A grant from the European Community, MRTN-CT-2004–005330 (to A. H., P. F. D., M. K.). The costs of publication of this article were defrayed in part by the payment of page charges. This article must therefore be hereby marked "*advertisement*" in accordance with 18 U.S.C. Section 1734 solely to indicate this fact.

[S] The on-line version of this article (available at http://www.jbc.org) contains supplemental Figs. 1–4.

[1] These authors contributed equally.

[2] Received support from a Short Term Scientific Mission from COST D22 action on lipid protein interactions and from the Berliner Chancengleichheits-Programm N-318/06.

[3] Supported by research grants from the CNRS (UMR 7099) and by Université Paris 7- Denis Diderot.

[4] To whom correspondence may be addressed. Tel.: 49-30-2093-8830; Fax: 49-30-2093-8585; E-mail: thomas.pomorski@rz.hu-berlin.de.

[5] To whom correspondence may be addressed. Tel.: 49-30-2093-8830; Fax: 49-30-2093-8585; E-mail: andreas.herrmann@rz.hu-berlin.de.

[6] The abbreviations used are: PC, phosphatidylcholine; CPM, 7-diethylamino-3-(4′-maleimidylphenyl)-4-methylcoumarin; ER, endoplasmic reticulum; GUV, giant unilamellar vesicles; LPC, L-α-lysophosphatidylcholine; PE, phosphatidylethanolamine; TE, Triton X-100 extract; RT, room temperature; NBD, 7-nitrobenz-2-oxa-1,3-diazol-4-yl; C6-acyl-PC, 1-acyl-2-hexanoyl-*sn*-glycero-3-PC; C6-NBD-PC, 1-palmitoyl-2-(NBD-hexanoyl)-*sn*-glycero-3-PC.

bilayer equilibration of the inserted lipids. The time dependence of shape changes could be used for derivation of the flip-flop rate constant.

Here we demonstrate by reconstitution of yeast ER flippase activity into GUVs that dynamics of GUV shape changes can serve as a tool for quantitative characterization of the lipid transport activity of flippases (Fig. 1*B*). In this case the characteristic time of the sequential shape transformation of protein-containing GUVs is on the order of flip-flop of spin-labeled and fluorescent phospholipid analogues found previously in microsomes (7). The major advantage of this approach compared with the previous ones is the use of unlabeled lipids, which allows avoiding possible artifacts related to the utilization of lipid analogues with bulky reporter moieties (9).

EXPERIMENTAL PROCEDURES

Materials—Egg L-α-lysophosphatidylcholine (egg-LPC), egg phosphatidylcholine (egg-PC), egg phosphatidylethanolamine (egg-PE), and dioleoylphosphatidylglycerol (PG) were from Sigma-Aldrich. 1-Acyl-2-hexanoyl-*sn*-glycero-3-phoshatidylcholine (C6-acyl-PC) was synthesized from egg-PC (15). C6-ceramide, C16-ceramide, and galactosylceramide were synthesized according to López-Montero *et al.* (11). 7-Diethylamino-3-(4′-maleimidylphenyl)-4-methylcoumarin (CPM), BODIPY FLC_5-PC and -Cer were purchased from Molecular Probes (Eugene, OR).

Yeast Strains and Culture Conditions—The yeast strain *sec61* (*MATα ura3-52 leu2-3-112 ade2-10 sec61ts*) obtained from J. Holthuis (University Utrecht, The Netherlands) was used. Microsomal membranes containing a green fluorescent protein-tagged transmembrane domain linked to carboxypeptidase yscY (for details, see Ref. 16) were derived from W303-1C Δ*der3* (*MATα ade2-1 ura3-1 his3-11, 15 leu2-3, 112 trp1-1 can1-100 prc1-1,* Δ*der3*::*HIS3*) harboring the plasmid pMA1 (kindly provided by D. Wolf, University Stuttgart, Germany). Strains were grown at 27 °C in liquid YPD medium (1% Bacto yeast extract, 2% Bacto peptone (Difco, 2% glucose). The strain W303-1C Δ*der3* harboring pMA1 was grown in the absence of uracil in synthetic complete medium with 2% glucose at 27 °C. Cells were harvested in the exponential phase, and growth was monitored by A_{600}.

Microsome Preparation—Microsomes were prepared essentially according to Zinser and Daum (17). Briefly, cells were pretreated with 10 mM dithiothreitol in 100 mM Tris sulfate (pH 9.4) for 10 min, incubated with Zymolyase-100T (ICN Biomedicals, Eschwege, Germany) at 5 mg/g of cells (wet weight) in buffer (20 mM potassium phosphate (pH 7.2), 1.2 M sorbitol) at 30 °C for 30 min, harvested, and then lysed in homogenizing buffer (10 mM Tris-HCl (pH 7.4), 0.6 M sorbitol) containing protease inhibitors (1 mg/ml aprotinin, 1 mg/ml leupeptin, 1 mg/ml pepstatin A, 5 mg/ml antipain, 1 mM benzamidine, 1 mM phenylmethylsulfonyl fluoride) using a Dounce homogenizer with a tight-fitting pestle. The cell lysate was centrifuged at 3000 × *g* for 5 min. The pellet was resuspended in homogenizing buffer, homogenized, and centrifuged as above. Both supernatants were pooled. Membrane pellets from differential centrifugation (9,000 × *g* for 10 min, 20,000 × *g* for 30 min, 40,000 × *g* for 30 min, 100,000 × *g* for 45–75 min) were screened for organelle marker proteins by immunoblotting. The green fluorescent protein-tagged ER membrane protein became enriched in the 40,000 × *g* fraction. Pellets of 40,000 × *g* and 100,000 × *g* enriched in ER membrane proteins were resuspended in buffer T (10 mM Tris-HCl (pH 7.4), 1 mM EDTA) using a tight fitting Dounce homogenizer and stored at −80 °C. If not stated otherwise, the 100,000 × *g* fraction was used for further preparation of proteoliposomes.

Preparation of Proteoliposomes—Microsomal fractions (20 mg/ml protein) were solubilized by diluting half with 1.6% (w/v) Triton X-100 (Roche Diagnostics) in buffer T. After incubation for 45 min on ice, insoluble material was removed by centrifugation (177,000 × *g*, 30 min, 4 °C). The resulting supernatant is designated as Triton extract (TE). For reconstitution, egg-PC in chloroform was dried under nitrogen in a glass tube and then dissolved in buffer TX (10 mM Tris-HCl (pH 7.4), 1 mM EDTA, 0.8% w/v Triton X-100) to a final concentration of 4.5 mM. Various amounts of TE were added to generate proteoliposomes with different lipid/protein ratios. Protein-free liposomes were prepared similarly by substituting buffer for TE. To remove detergent and generate vesicles, 100 mg of SM2 BioBeads (Bio-Rad) per 1 ml of solution were added. After 3–4 h rotating at room temperature (RT), the samples were supplemented with an additional 200 mg/ml of BioBeads and transferred to 4 °C for further 14–16 h of mixing. Turbid suspensions were withdrawn, carefully avoiding collection of any beads, and adjusted to an 8–10-fold excess of buffer T. The vesicles were collected by centrifugation (200,000 × *g*, 50 min, 4 °C) and resuspended at 9 mM phospholipid using a Dounce homogenizer. Protein recovery in the reconstituted vesicles was about 30–45%; lipid recovery was about 90%. More than 99.9% of the original Triton X-100 was removed, as determined by extraction with four volumes of chloroform/methanol (1/2, v/v) and subsequent measurement of the supernatant at A_{275}.

To label microsomal proteins before reconstitution, 450 μl of TE (0.9 mg protein) were mixed with 20 μl of a 10 mM Me_2SO solution of the thiol-reactive fluorescent probe CPM and incubated at 4 °C overnight in the dark. Unbound label was removed by dialysis. Analysis by SDS-PAGE and thin layer chromatography demonstrated that at this temperature only proteins but no membrane lipids became labeled (data not shown).

Virosome Preparation—Virosomes were prepared from influenza viruses (strain X31) essentially as described for proteoliposomes. A mixture of virosomal TE, Triton X-100-solubilized egg-PC, and egg-PE (14.75/0.275, w/w) was used for reconstitution at lipid/protein ratio of 20 (w/w). To visualize reconstitution of viral proteins, viruses were preincubated for 2 h at RT in the dark with CPM, added from 5 mM Me_2SO stock to molar excess of 10 over hemagglutinin. To remove uncoupled CPM, labeled viruses were washed twice in phosphate-buffered saline (pH 7.4) and harvested by centrifugation at 45,000 × *g*. SDS-PAGE analysis revealed that only influenza virus hemagglutinin was labeled (data not shown).

Preparation of Giant Unilamellar Vesicles—GUVs were generated from proteoliposomes by the electroformation technique in a chamber made of indium-tin-oxide-coated glass slides at RT (18–20). The oscillating electric field that was

applied only during GUV formation did not affect the activity of membrane proteins (20). For GUVs consisting only of lipids, 70 μl of lipid solution in chloroform (0.25 mg/ml) were deposited in small droplets onto each slide. Subsequently, solvent was evaporated in a desiccator (10 mbar) for 60 min at RT. To prepare GUVs with reconstituted proteins according to Girard *et al.* (20), proteoliposomes were diluted with distilled water to 0.4–0.8 mg/ml lipid, and 25–50 μl of this suspension was deposited onto each glass slide in small droplets. To avoid denaturation, proteoliposomes were dehydrated only partially by placing glass slides in a sealed chamber containing a saturated NaCl solution. After overnight incubation a film had formed on the glass slides.

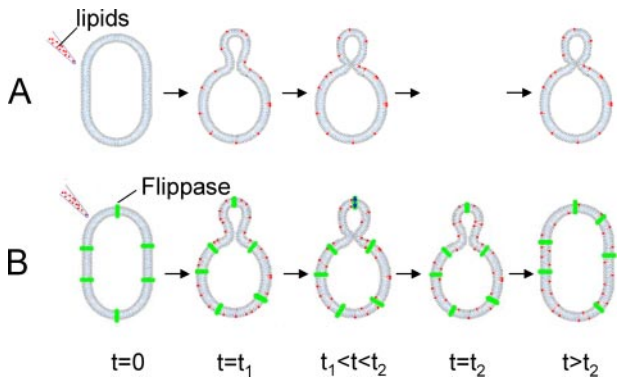

FIGURE 1. **Flip-flop of phospholipids assessed by shape changes of egg-PC GUVs.** Insertion of exogenously added phospholipids (*e.g.* egg-LPC) at $t = 0$ into the outer leaflet caused budding. In the absence of rapid lipid flip-flop, the bud remained essentially stable (*A*; see Fig. 2), whereas in the presence of a rapid spontaneous or flippase-mediated lipid flip-flop (*B*), the bud retracts, and the GUV returned to its original shape (see Fig. 4). At t_1 bud formation is observed, whereas recovery of the original shape begins at t_2 (see "Results").

Subsequently, the chamber was assembled by sealing both glass slides with silicon paste. The sucrose solution (250 mM sucrose, 0.02% NaN_3) was injected with a syringe (about 1 ml) through a micropore filter immediately before connecting the completely sealed chamber to the generator. The voltage of the applied AC-field was increased stepwise every 6 min from 20 mV up to 1.1 V while continuously increasing the frequency from 4 to 10 Hz within the first minute. The AC field was applied for 3–12 h. To complete the procedure voltage was raised to 1.3 V, and the frequency was lowered to 4 Hz for 1 h. The chamber was then stored in a refrigerator at 4 °C.

Observation and Analysis of GUV Shape Changes—Spherical GUVs cannot undergo shape changes due to the minimized surface to volume ratio. Therefore, deflated vesicles appropriate for shape change studies (11) were achieved osmotically by transferring 10–50 μl of GUVs into 150 μl of a glucose solution (275 mM glucose, 0.02% Na_3) on a microscope slide and allowing water to evaporate for 30–60 min at room temperature. To prolate GUVs, lipids that are known to incorporate rapidly into lipid bilayers were added. Typically, 10 μl of 0.1 mM lipid (typically egg-LPC) in glucose solution was injected (representing time zero in the shape changes analysis). The time points t_1 (begin of budding transition) and t_2 (begin of bud retraction) were measured by microscopic observation of GUV shapes for each experiment (see "Results"). All experiments were performed at room temperature. To determine the amount of lipid incorporated into GUVs, we used radioactive L-lyso-3-phosphatidylcholine,1-[1-^{14}C]palmitoyl (CFA633, Amersham Biosciences). 50 μl of GUVs were transferred to a microscope slide, and 150 μl of a glucose solution (275 mM glucose, 0.02% NaN_3) was added. After GUVs settled, radioactive lipids were added, and the suspension was incubated for up to 2 h. Subsequently, aliquots from the supernatant were taken, and radioactivity was measured.

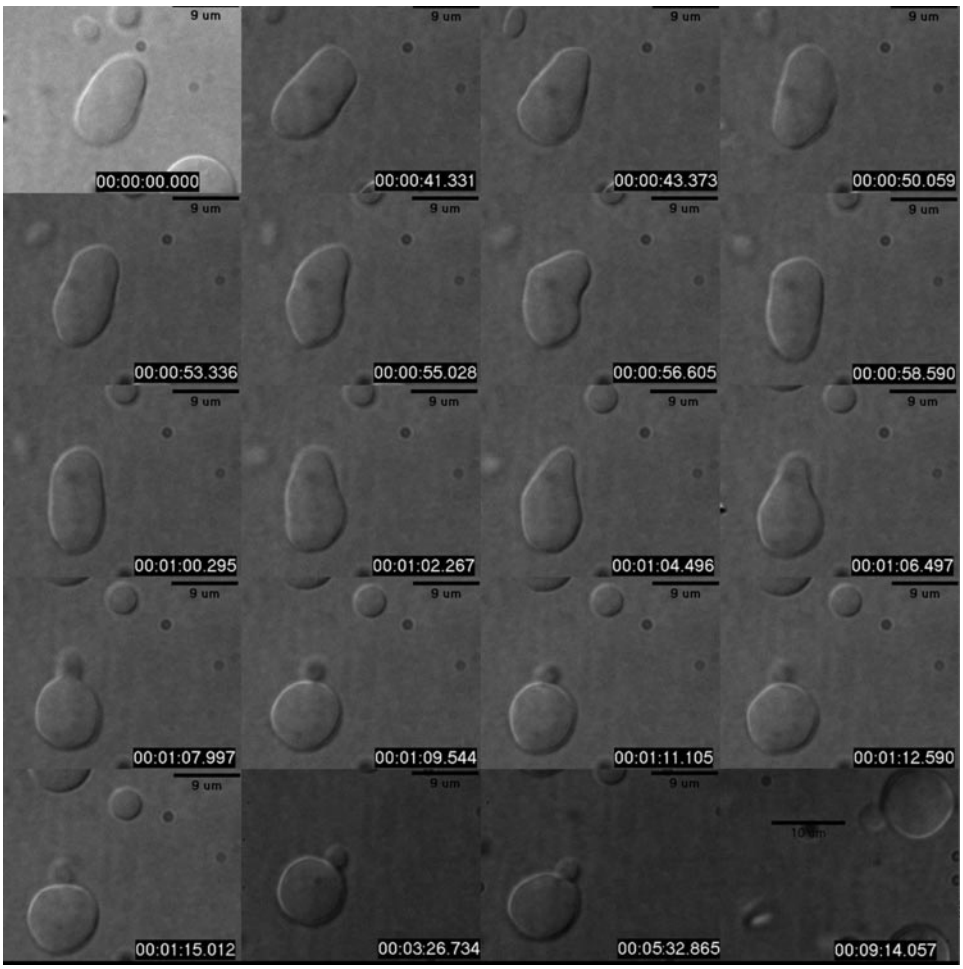

FIGURE 2. **Shape transition of egg-PC GUVs upon the addition of egg-LPC.** Insertion of egg-LPC into the outer leaflet caused the formation of a stable bud that did not retract in the time course of the experiment (for details, see "Experimental Procedures").

Miscellaneous—Protein content was quantified after TCA precipitation using micro-BCA Protein Assay reagent (Pierce) and BSA as a standard. Phospholipid content was determined by extracting lipids according to Bligh and Dyer (21) and measuring the amount of phospholipid phosphorus (22).

RESULTS

Shape Changes of Protein-free GUVs—Insertion of unlabeled lipids such as egg-LPC, C6-acyl-PC, or C6-ceramide into the external leaflet of GUVs made of egg-PC resulted in formation of a bud-like structure (Figs. 1*A* and 2). If egg-LPC or C6-acyl-PC, which are known to undergo a very slow flip-flop like egg-PC, was added, the bud was stable (Fig. 2). Whereas if lipids were added that rapidly redistribute between the two membrane leaflets, *e.g.* ceramide, the initial bud was reversible, and the prolate shape was recovered (11). This can be explained by a decline in the monolayer area difference due to the transbilayer equilibration of inserted lipids. Bud formation was also reversible when egg-LPC was added to egg-PC GUVs containing already a lipid that flips rapidly, such as the long chain C16-ceramide (5 mol %) (not shown). When ceramide was replaced by the slow flipping galactosylceramide, the prolate shape was not recovered after 1 h. The experiments with ceramide and egg-LPC prove that the transversal diffusion of an unlabeled lipid with a fast flip-flop rate can be measured in GUVs even disregarding the flipping ability of the added lipid. However, this conclusion may not be generalized. Although cholesterol is known to flip rapidly across the lipid bilayer (23, 24), Mathivet *et al.* (19) did not observe retraction of the initial bud formation when egg-LPC was added to egg-PC GUVs containing up to 23 mol % of cholesterol. A possible explanation could be that transbilayer redistribution of cholesterol cannot compensate for area asymmetry due its specific molecular properties, *e.g.* it is known that cholesterol cannot form bilayers.

To substantiate our conclusions on lipid translocation drawn from GUV shapes, we chose further processes exploiting microscopic visualization of GUV behavior. First, Cullis and co-workers (Ref. 25 and publications cited therein) demonstrated that pH gradients influence the distribution of charged phospholipids as phosphatidylglycerol (PG) across the membrane of unilamellar 100-nm vesicles. Using various assays they could prove that PG flips rapidly in its neutral form, whereas it is sequestered within one membrane leaflet in the case of deprotonation in contact with basic environment. Thereby, arising transversal asymmetry could clearly be related to membrane curvature and molecule balance between the leaflets in GUVs (13). When prolate GUVs from egg-PC containing 1 mol % of dioleoyl-PG are exposed to an increased pH (from pH 7 to 9) in the surrounding medium by the addition of NaOH, spontaneous migration of PG from the inner leaflet (pH 7) to the exterior (pH 9) results in relative immobilization due to their acquired head-group charge. The excess molecules account for an area imbalance that is apparent from an instantaneous budding transition (Fig. 3*A*). The connecting neck is progressively elongated during the following minutes, eventually forming a tether with a highly mobile daughter vesicle (see the change of focus to resolve both structures in last images of series). Control GUVs from egg-PC maintain their prolate shapes for more than 10 min (not shown). By a second independent approach we proved directly that shape changes indeed correlate with the transbilayer distribution of externally added lipids using BODIPY-labeled PC and Cer (see supplemental Fig. 1). Quantification of the fluorescent fraction on the inner surface of the membrane, as determined by protection from trypan blue quenching, is displayed in Fig. 3*B*. BODIPY-PC proves to be confined essentially to the outer leaflet, whereas the distribution of the Cer analogue resembles that of GUVs prepared with a symmetric BODIPY-PC distribution between both leaflets. We, therefore, conclude that lipid distribution affects the membrane curvature of GUVs, and its dynamics can be reliably visualized as shape changes.

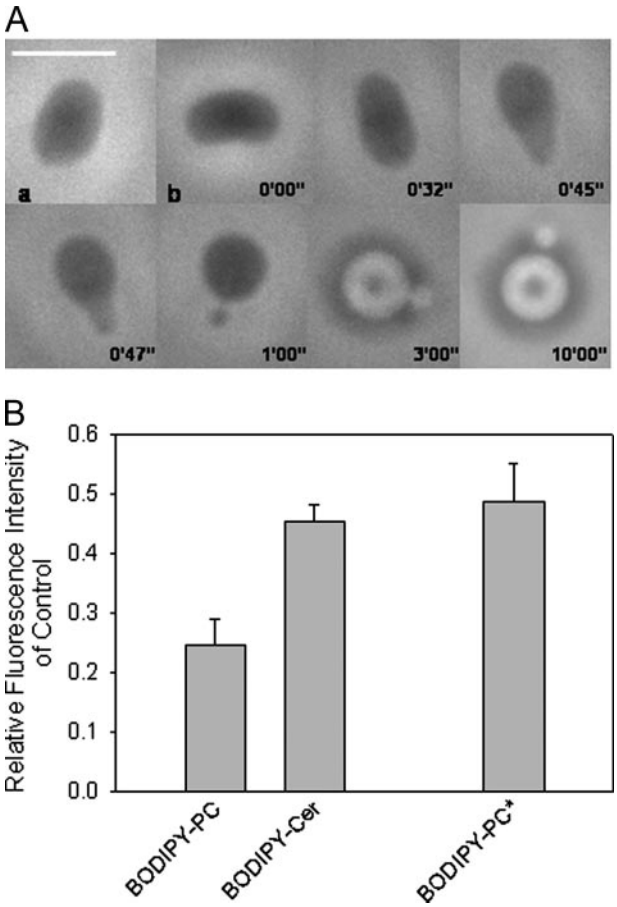

FIGURE 3. **Shape changes of GUVs correlate with transbilayer redistribution of lipids.** *A*, shape changes with pH-induced flip-flop of phosphatidylglycerol. GUVs were prepared from egg-PC containing 1 mol % dioleoylphosphatidylglycerol. Shown is prolate GUV at pH 7 (*a*) subjected to pH increase (pH 9) by adding ~10 μl of NaOH (0.5 N) to ~400 μl of neutral glucose solution in the observation chamber (*b*). Phase contrast images are taken with respect to time of alkaline addition (0′00″); the *bar* corresponds to 10 μm. *B*, assessment of transbilayer distribution of BODIPY-PC and BODIPY-Cer after shape transitions. BODIPY-PC or -Cer were added to GUVs and incubated for 30 and 10 min, respectively. Subsequently, fluorescence intensities in the absence and presence of the quencher trypan blue (0.0075% w/v) were measured (as described in the supplemental data). Intensity in the absence of trypan blue was set to 1. For comparison, results for GUVs symmetrically labeled with BODIPY-PC are shown (*BODIPY-PC**). Data shown are the means ± S.E. of four determinations. Note that fluorescence intensities in the presence of trypan blue do not correlate in a quantitative manner with transbilayer distribution of BODIPY-lipids. For that, higher concentrations of the quencher would be necessary. However, such concentrations affect the stability of the GUVs.

Shape Changes of GUVs with Reconstituted ER Proteins—The flippase activity of yeast ER was first reconstituted into proteo-

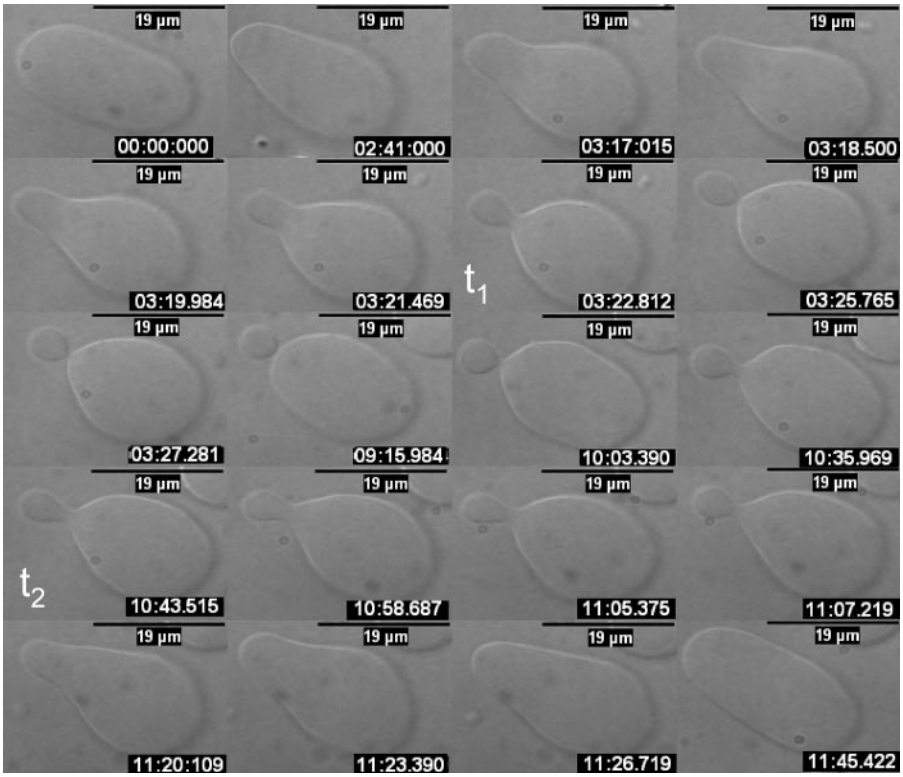

FIGURE 4. **Shape transition of GUVs prepared from proteoliposomes containing microsomal membrane proteins (100,000 × *g* fraction).** At time $t = 0$, egg-LPC was added. GUVs were visualized by differential interference contrast at RT. The lipid/protein ratio was 35/1 (w/w). The budding transition was observed at t_1 = 3:25 min. Recovery of the prolate shape started at t_2 = 10:35 min.

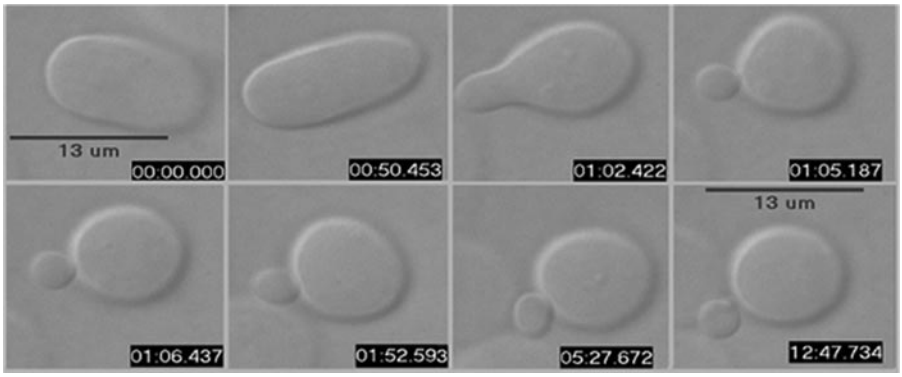

FIGURE 5. **Shape transition of GUVs prepared from virosomes containing influenza hemagglutinin.** Viral proteins were reconstituted in proteoliposomes containing egg-PC and egg-PE at a lipid/protein ratio of 20/1 (w/w). At time $t = 0$, egg-LPC was added. GUVs were visualized by differential interference contrast microscopy at RT.

liposomes as already described previously for rat liver (6, 7) and yeast ER (26). Applying established assays for measuring transbilayer movement (see Ref. 9 and references therein) confirmed protein-mediated flip-flop of fluorescent phospholipid analogues such as 1-palmitoyl-2-(NBD-hexanoyl)-*sn*-glycero-3-phosphocholine (C6-NBD-PC) being on the order of a minute.[7] Subsequently, GUVs were prepared from such proteoliposomes. No significant difference between the size of protein-free and protein-containing GUVs was found (not shown).

When egg-LPC or C6-acyl-PC was added, reconstituted GUVs budded within the first 5 min after injection of lipids and subsequently regained the prolate shape within 5–10 min (Fig. 4). We conclude that the reconstituted ER flippase activity triggers the rapid flip-flop that diminishes the surface area difference between the two leaflets. To demonstrate that GUVs undergoing reversible shape changes contain ER proteins, we reconstituted the ER fraction from a yeast strain expressing an ER resident, green fluorescent protein-tagged membrane protein as well as prelabeled TE (supplemental Figs. 3 and 4).

Shape Changes of GUVs Reconstituted with Influenza Virus Protein—To address whether the flippase activity is a property of specific membrane proteins (27), we studied shape changes of GUVs prepared from reconstituted influenza virosomes. Upon the addition of egg-LPC, GUVs formed stable buds (Fig. 5). This indicates that no significant flip-flop has occurred compensating for the surface imbalance between the two leaflets. Hence, the presence of reconstituted membrane proteins *per se* is not sufficient to trigger rapid flip-flop. These results argue for the presence of specific proteins with a flippase activity in the ER in agreement with previous studies (28). Notably, the absence of a rapid flip-flop in viral hemagglutinin containing GUVs rules out flip-flop favoring artifacts due to influence of the electric field on proteins during vesicle formation.

Determination of Lipid Exchange Rates—To estimate the rates of lipid exchange mediated by flippase activity between membrane monolayers, we used the experimentally observed dynamics of shape changes upon lipid insertion into GUV membranes. For that, the relevant data from experiments are the time points t_1 and t_2 taken at definite onset of formation and disappearance, respectively, of a spherical bud, both measured from the moment of lipid addition to the aqueous solution surrounding the GUVs.

The GUV shapes are governed to a great extent by the relation of their membrane monolayers (11), where the area asymmetry η is defined as the ratio of area difference ΔA between the monolayers to the area A of the bilayer mid surface: $\eta = \Delta A/A$. Budding of a prolate GUV has been established to occur when the monolayer area asymmetry

[7] S. Vehring, A. Herrmann, and T. Pomorski, unpublished data.

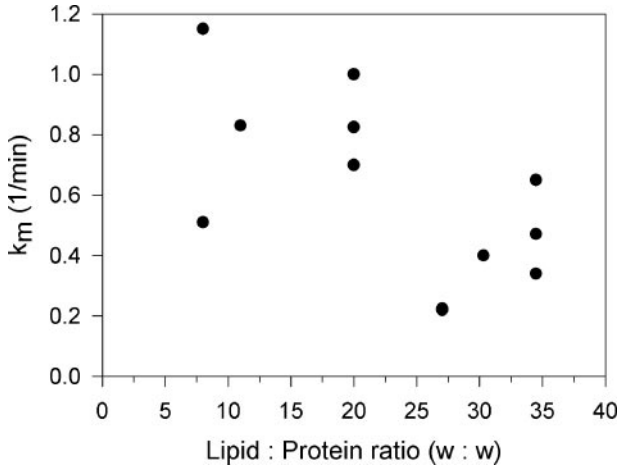

FIGURE 6. **The rate constant of flip-flop, k_m, of lipid in GUVs reconstituted from proteoliposomes containing different amounts of microsomal membrane proteins.** k_m was calculated according to the described model. One way analysis of variance revealed a significant influence of the lipid/protein ratio on k_m at a significance level of $\alpha = 0.1$ ($F_{Experiment} = 4.041 > F(3, 6, 0.01) = 3.29$; $F = 4.041$ corresponds to $\alpha = 0.069$).

TABLE 1

Shape transition times and estimated rate constants for reconstituted GUVs with varying lipid/protein ratio (L/P (w/w))

The times of formation, t_1, and disappearance, t_2, respectively, of a spherical bud were measured experimentally as described (at $t = 0$ lipids were added to the aqueous solution surrounding the GUVs). The fitted parameters are: J, lipid flux from surrounding solution into the outer monolayer; k_w, rate constant of the egg-LPC transfer from the membrane monolayers to the surrounding solution; k_m, rate constant of the intermonolayer lipid exchange; k_c, rate constant of egg-LPC transfer from the internal aqueous solution into the inner monolayer; b, scaling factor proportional to A/V, characterizing the linear dimension of the vesicle; L/P, the lipid/protein ratio (w/w).

L/P ratio	t_1	t_2	Ja/k_w	k_w	k_w	k_cb
	min	*min*		min^{-1}	min^{-1}	min^{-1}
8	01:43	02:02	0.033	0.03	1.150	0.028
8	03:11	16:08	0.026	0.03	0.510	0.007
11	02:18	07:12	0.033	0.03	0.830	0.015
20	01:52	04:06	0.033	0.03	1.000	0.020
20	01:30	07:30	0.033	0.03	0.825	0.015
20	02:11	08:17	0.033	0.03	0.720	0.010
27	10:50	13:05	0.013	0.03	0.225	0.003
27	12:25	27:00	0.013	0.03	0.220	0.003
30	05:03	20:00	0.023	0.03	0.400	0.004
35	03:25	10:35	0.033	0.03	0.650	0.007
35	06:00	19:00	0.033	0.03	0.340	0.003
35	05:15	09:48	0.026	0.03	0.471	0.004

exceeds 0.1%, *i.e.* $\eta \cong 0.001$ (11, 12). Accordingly, t_1 and t_2 correspond to $\eta \cong 0.001$.

Our analysis includes three sequential tasks; (i) to model theoretically the kinetics of redistribution of exogenously added lipids between the aqueous solution and the GUV membranes; (ii) to express the time of reaching an area asymmetry of 0.1% through the kinetic parameters of the system; (iii) to determine these parameters based on the experimentally measured values of t_1 and t_2. Within the same kinetic scheme, the present analysis takes into account transbilayer flip-flop as well as lipid exchange between the membrane and the aqueous solutions inside and outside of the vesicle. This provides for self-consistent determination of all kinetic constants exclusively based on the available measurements with unlabeled lipids. In this regard our model advances the one recently proposed for evaluation of the flip-flop rate on the basis of GUV shape changes (11).

The detailed kinetic scheme describing our system is presented and analyzed in the Appendix. Characterizing the time dependence of the area asymmetry η, the major parameter is the rate k_m of lipid flip-flop between both monolayers. Determination of k_m requires knowledge of three other system parameters related to the egg-LPC exchange rates between the membrane and the aqueous solution (see "Appendix").

To illustrate quantitative determination of k_m, the time points t_1 and t_2 were taken from microscopic observations presented in Fig. 4 (see images taken for t_1 and t_2). With 3:25 min (t_1) and 10:35 min (t_2) we obtained values of 0.3 min^{-1} for k_m and 2.3 min for the corresponding half-time, respectively.

In Fig. 6 k_m is plotted *versus* the lipid/protein ratio of the vesicle membrane. Despite the considerable scattering, it displays apparent increase of flip-flop with protein content. These values are on the order of those that have been measured for flip-flop of fluorescently labeled phospholipid analogues in the ER of eukaryotic cells with lipid/protein relations on the order of 0.03 (w/w) (see "Discussion").

From the images shown in Fig. 4, the accuracy of determination t_1 and t_2 is on the order of 10 s. Variation of this order has only a very minor influence on calculation of k_m (see Table 1 and supplemental data). In this regard, an accuracy of ≥1 min would cause a variation of k_m of ≥20% (see the three examples at the bottom of Table 1 and supplemental data).

DISCUSSION

The present study demonstrates that GUVs and their shape changes provide a suitable tool to characterize protein-mediated lipid transport across the bilayer. We have shown that the flippase activity of yeast ER enabling rapid phospholipid translocation can be reconstituted in GUVs. The shape change assay independently supports previous studies showing that the spontaneous translocation rates of lyso-PC (29, 30) and ceramide (11, 31) differ distinguishably. Therefore, the assay has been applied to flippase protein containing GUVs. The flippase activity was inferred from the reversibility of bud formation triggered by the insertion of added lipids into the external leaflet of prolate GUVs. The half-time of phospholipid flip-flop deduced from the recovery of the original prolate shape was on the order of few minutes, which is indeed very similar to half-times that have been measured by a back exchange assay for the flippase-mediated translocation of fluorescent phospholipid analogues in the ER of eukaryotic cells and in the inner plasma membrane of bacteria. For instance, Marx *et al.* (7) reported for flip-flop of the fluorescently short chain-labeled phospholipid analogues C6-NBD-PC and C6-NBD-PE in rat liver microsomes half-times of about 1.5 and 2.5 min, respectively. In the same order is the half-time of C6-NBD-PC in microsomes of yeast[7] as used here for preparation of GUVs. Likewise, in inner membrane vesicles from *Escherichia coli*, the half-time for the transbilayer movement of C6-NBD-PE was between 1 and 3 min (32). Although in the latter studies the fast flip-flop could only be probed by labeled analogues, assessment by shape changes of GUVs allows avoiding bulky reporter moieties and can, therefore, be applied to lipids resembling endogenous molecules much better. Moreover, the physicochemical conditions at GUV membranes, which are disposed to flexible reaction to a

small molecular excess, offer investigation of lipid translocation with minimal perturbation of the bilayer.

Flippase activity in the ER microsomes and inner membrane of bacteria is rather unspecific and triggers a fast flip-flop of various (phospho)lipid analogues (5, 6, 8, 26–28, 32–34). Therefore, we cannot discriminate between flip-flop of exogenously added lipids (egg-LPC) and intrinsic lipids as additionally indicated by results with GUVs containing rapidly flipping ceramide. Typical flip-flop of LPC is very slow and not substantially different from that of phospholipids bearing two long fatty acid chains (29, 30). Thus, we surmise that flip-flop of all lipids present in GUVs is mediated by the flippase.

Flippase Versus Membrane-spanning Helices Induced Translocation of Phospholipids—Transbilayer movement in biogenic membranes as eukaryotic ER or prokaryotic plasma membrane is fast, with flip-flop half-times on the order of minutes or less. Kol *et al.* (27, 33) found that certain single α-helical membrane-spanning peptides promote transbilayer movement of some phospholipid classes in synthetic membranes, suggesting that lipid flip-flop proceeds in the absence of a dedicated flippase.

Our study clearly demonstrates that the presence of membrane proteins in GUVs *per se* is not sufficient to facilitate flip-flop of phospholipids. As shown for reconstituted influenza virus hemagglutinin, which exists as a trimer representing three transmembrane domains, the bud formation in GUVs by externally inserted egg-LPC was irreversible, indicating the absence of a rapid flip-flop. Thus, our results argue for the presence of specific proteins (flippases) facilitating a fast transbilayer movement of lipids in the ER. This conclusion supports recent studies on the ER from rat liver cells suggesting the existence of dedicated flippases. In an attempt to identify the flippase(s) of microsomal membranes, Menon *et al.* (28) reconstituted protein fractions separated either on a glycerol gradient or by anion exchange chromatography into proteoliposomes. This approach yielded protein pools of enriched flip-flop activity, suggesting that specific proteins are responsible for the fast lipid movement in the ER.

Although our study and others suggest the presence of flippases, it does not preclude that membrane spanning α-helices may promote transbilayer movement of lipids as found by Kol *et al.* (27, 33). However, flip-flop half-times reported therein were significantly longer in comparison to those observed for biogenic membranes in native state as well as fractionated reconstituted into proteoliposomes.

Our study and previous efforts (26, 28) have shown that the flippase activity can be extracted by Triton X-100. Under our conditions, about 10% of ER proteins are solubilized from yeast ER, of which about 40% could be reconstituted. Recently, we have studied the flippase activity in reconstituted ER proteoliposomes (for preparation, see "Experimental Procedures") as a function of the protein to lipid ratio using the fluorescent lipid analogue C6-NBD-PC.[7] Based on the obtained dose-response curve and assuming that the inflection point toward saturation reflects the situation where every vesicle would be equipped with at least one flippase, we deduced the abundance of functional flippases as follows: (i) the average proteoliposome diameter of 200 nm (electron micrographs[7]) gives with a cross-sectional area of 0.6 nm^2 for PC 1.4×10^{18} vesicles/mol of phospholipid; (ii) the obtained inflection at about 8 g/mol gives with (i) 5.7×10^{-18} g of protein/vesicle; (iii) with an average molecular mass of 50 kDa for ER proteins (Ref. 35),[7] the initial assumption finally results in a mass proportion for flippase protein of 1.5% of ER extract reconstituted in GUVs. Very likely, flippase proteins constitute a minor fraction of ER proteins. Although the lipid/protein ratio in yeast microsomes (~0.03 w/w) is about 2 orders of magnitude lower compared with that of proteoliposomes and GUVs (see Table 1 and Fig. 6), the rapid flip-flop in GUVs indicates that the majority of flippase proteins if not all could be recovered in GUVs. Because the molecular identity of flippase proteins is not yet known, we cannot provide an estimate of how many flippase proteins have been reconstituted into GUVs and to which extent this reconstituted system corresponds to native ER membranes regarding this condition.

Application of GUVs to Energy-dependent Lipid Flippases—The present approach should also allow investigation of energy-dependent flippases. Although flippases are very likely reconstituted to a similar extent in both opposing directions, unidirectional lipid transport can be ensured by allowing ATP to access only one membrane leaflet. Characterizing the activity of energy-dependent flippases would not require the addition of lipids. Lipid species to be transported can already be incorporated during GUV assembly. Because of the unidirectional fashion of oriented lipid transport, area differences would be created leading to a shape change. This is different from the visualization of energy-independent flippase activity in GUVs where shape changes have to be triggered first, *e.g.* by supplementing the external leaflet with additional lipids.

Acknowledgments—We gratefully acknowledge Thomas Korte for excellent assistance in fluorescence microscopy, Patricia Bassereau for introduction into protein reconstitution, Bärbel Hillebrecht for help with virus preparation, and Dieter Wolf and Joost Holthuis for generously providing yeast strains and plasmid. Lara Kutschenko (University of Bonn) was a supported by the Studienstiftung des Deutschen Volkes.

APPENDIX

Kinetic Analysis of LPC Partitioning and Transmonolayer Area Asymmetry—Upon the addition of lipid, *e.g.* LPC, to the aqueous solution surrounding a GUV, lipids partition between the solution and the outer monolayer of the GUV membrane. In the presence of flippase activity, lipid redistribution occurs between the outer and the inner monolayer. And finally, LPC partitions between the inner membrane monolayer and the inner aqueous volume of the vesicle.

We characterize the system by the surface density of LPC in the outer and inner monolayer denoted by X and Y, respectively, the LPC aqueous concentration in the outer solution close to the vesicle membrane, c_0, and the LPC concentration in the internal volume of the vesicle, c_{in}. Before insertion of LPC, the areas of the outer, A_{out}, and inner, A_{in}, monolayers of GUV are equal, $A_{out} = A_{in} = A$. In the course of LPC partitioning, these areas become

$$A_{out} = A \cdot (1 + aX) \qquad \text{(Eq. 1)}$$

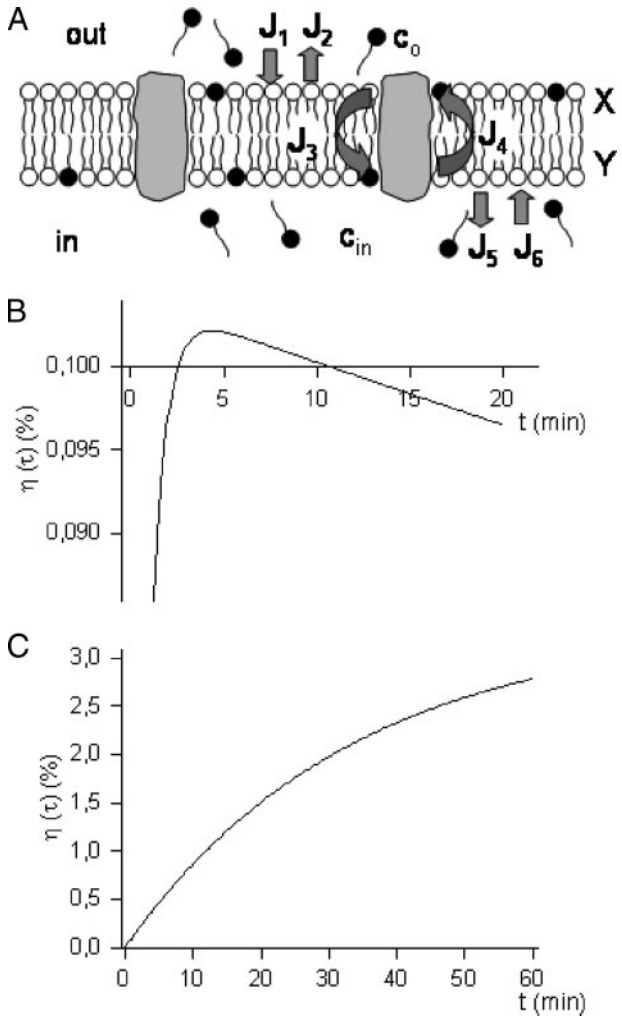

FIGURE 7. **Model for theoretical determination of lipid exchange rates.** *A*, model. Dependence of monolayer area asymmetry $\eta = \Delta A/A$ (in %) upon insertion of exogenously added lipids into the outer leaflet ($t = 0$) in the presence (*B*) and absence (*C*) of flip-flop. GUV budding has been established to occur when η equals ~0.1% ($\eta \approx 0.001$) as indicated in *B*. For details, see "Results."

and

$$A_{in} = A(1 + aY), \qquad \text{(Eq. 2)}$$

where a is the LPC molecular area. The emerging monolayer area asymmetry is

$$\eta = \frac{A_{out} - A_{in}}{A} = a(X - Y). \qquad \text{(Eq. 3)}$$

We assume that the monolayer area asymmetry remains small, $|\eta| \ll 1$, and in all the equations below, we account only contributions of the first non-vanishing order in η.

To describe the entire redistribution process we consider six lipid fluxes illustrated in Fig. 7*A*; (i) from the outer solution into the outer membrane monolayer,

$$J_1 = J = k_c c_0, \qquad \text{(Eq. 4)}$$

where c_0 is the LPC aqueous concentration in the vicinity of the membrane surface, and k_c is the water-membrane exchange rate constant; (ii) from the outer monolayer back to the surrounding aqueous solution,

$$J_2 = k_w X, \qquad \text{(Eq. 5)}$$

where k_w is the membrane-water exchange rate constant; (iii) from the outer to the inner membrane monolayer,

$$J_3 = k_m X, \qquad \text{(Eq. 6)}$$

where k_w is the rate constant of lipid exchange between the monolayers; (iv) from the inner back to the outer monolayer,

$$J_4 = k_m Y, \qquad \text{(Eq. 7)}$$

(v) from the inner membrane monolayer to the inner aqueous solution of the vesicle,

$$J_5 = k_w Y, \qquad \text{(Eq. 8)}$$

(vi) from the inner solution back to the inner membrane monolayer,

$$J_6 = k_c c_{in}, \qquad \text{(Eq. 9)}$$

where c_{in} is the inner aqueous concentration of LPC next to the membrane. The rate constants k_w, k_c, and k_m and their units are defined according to the standard Langmuir approach to description of molecular exchange between a surface and a volume phase or between two surfaces (36, 37).

Equations 2–5 do not account for the influence of elastic stresses on the lipid fluxes, which can emerge within the membrane monolayers as a result of the monolayer area asymmetry. Estimations show that for realistic values of η, the elastic stress effects provide negligible corrections to Equations 2–5. Moreover, we describe the lipid fluxes between the monolayers, J_3 and J_4, by the same rate constant k_m. This implies that the rate constants are not affected by monolayer bending, which can be justified for the large membranes of GUVs but may be invalid for small lipid vesicles.

The redistribution between the various compartments results in time evolution of the LPC concentrations within the monolayers, X and Y, and in the aqueous compartments, c_0 and c_{in}. In our system the outer aqueous volume is very large compared with the volume enclosed by GUVs. Therefore, only a small fraction of the total lipid will be incorporated into the vesicles, meaning that the change of the outer aqueous concentration of LPC can be considered as a constant, c_0 = constant. Indeed, by using radioactive L-lyso-3-phosphatidylcholine, 1-[1–^{14}C]palmitoyl (see "Experimental Procedures"), we found that after 2 h of incubation of GUVs, only 11% of added lipids were incorporated. A similar value can be estimated on the basis of the water/lipid partition coefficient of lysolecithin (monopalmitoyl), which is $K_p \approx 0.5 \times 10^{-6}$ (38). Depending on the amount of GUVs (see "Experimental Procedures"), between 13 and 4% of lipids will be incorporated.

The dependence on time of the three other concentrations, X, Y, and c_{in}, is determined by the following equations.

$$\frac{dX}{dt} = J_1 - J_2 - J_3 + J_4 = J - k_w X - k_m X + k_m Y, \qquad \text{(Eq. 10)}$$

$$\frac{dY}{dt} = J_3 - J_4 - J_5 + J_6 = k_m X - k_m Y - k_w Y + k_c c_{in}. \quad \text{(Eq. 11)}$$

To obtain the equation for the time dependence of the LPC concentration in the lumen of vesicles, c_{in}, we have to take into account that variation of the total number of LPC molecules in the vesicle lumen, Vc_{in}, is determined by the balance between the total number of molecules entering and leaving the lumen, AJ_5 and AJ_6, respectively, per unit time (recall, that V and A are the vesicle volume and the area of the inner monolayer, respectively; the fluxes J_5 and J_6 are determined as the number of LPC molecules exchanged per unit time and unit monolayer area). The resulting equation is,

$$\frac{dc_{in}}{dt} = (J_5 - J_6)b = (k_w Y - k_c c_{in})b. \quad \text{(Eq. 12)}$$

where $b = A/V$ has the unit of inverse length to account for the fact that molecules (LPC) exchange between a volume and an area (monolayer) characterized by concentration and surface density. Solution of this system of equations has to take into account the initial concentration of LPC in the membrane layers and the internal vesicle volume, respectively, to be zero: $X(t = 0) = 0$, $Y(t = 0) = 0$, $c_m(0) = 0$.

We consider two types of solution of Equations 10–12 as relevant for our experimental setup. In a bilayer containing flippases, the rate of lipid exchange between the monolayers has to be high compared with the off rates of LPC from the membrane either to the aqueous medium or to the vesicle lumen, $k_m \gg k_w$ and $k_m \gg k_c b$, respectively. The time evolution of the monolayer area asymmetry is given in this case by

$$\eta(t) = \frac{Ja}{2k_m}\left(\left(1 + \frac{k_c b}{k_w}\right)e^{-\frac{k_c b}{2}t} - \left(1 + \frac{k_c b}{2k_w}\right)e^{-2k_m t} - \left(\frac{k_c b}{2k_w}\right)e^{\left(-k_w - \frac{k_c b}{2}\right)t}\right) \quad \text{(Eq. 13)}$$

In the absence of flippases, the transfer of LPC between the monolayers is very slow, $k_m \ll k_w$, and effectively LPC partitions only between the external solution and the outer membrane monolayer. Then the related time evolution of the area asymmetry is given by

$$\eta(t) = \frac{Ja}{k_w}(1 - e^{-k_w t}). \quad \text{(Eq. 14)}$$

Determination of Kinetic Parameters—Time behavior of the monolayer area asymmetry, η, in the presence of flippases given by Equation 13 has a non-monotonic character, as illustrated in Fig. 7*B*. The initial increase of η corresponds to redistribution of egg-LPC between the external solution and the membrane monolayers, whereas the decrease of η with time results from egg-LPC partitioning into the internal vesicle volume and equilibration throughout the whole system. The time points of bud formation, t_1, and decay, t_2, are represented by intercepts of the curve $\eta(t)$ with the line $\eta = 0.001$ (Fig. 7*B*). Fitting of these intercept points to the experimental values of t_1 and t_2 gives two equations for the parameter determination: $\eta(t_1) = 0.001$ and $\eta(t_2) = 0.001$.

TABLE 2

Sensitivity of k_w and $k_c b$ with respect to variation of k_w (fixed *Ja*) and *Ja* (fixed k_w) for t_1 = 3:25 min, t_2 = 10:35 min (see Fig. 4)

The fitted parameters are: *J*, lipid flux from surrounding solution into the outer monolayer; k_w, rate constant of the egg-LPC transfer from the membrane monolayers to the surrounding solution; k_m, rate constant of the intermonolayer lipid exchange; k_c, rate constant of egg-LPC transfer from the internal aqueous solution into the inner monolayer; *b*, scaling factor proportional to A/V, characterizing the linear dimension of the vesicle.

Ja	k_w	k_m	$k_c b$
min^{-1}	min^{-1}	min^{-1}	min^{-1}
0.001	0.01	0.713	0.003
0.001	0.02	0.636	0.004
0.001	0.03	0.610	0.005
0.001	0.04	0.595	0.006
0.001	0.05	0.575	0.0063
0.001	0.06	0.564	0.0066
0.0006	0.03	0.45	0.012
0.0008	0.03	0.52	0.007
0.0010	0.03	0.61	0.005
0.0012	0.03	0.68	0.003

In the absence of flippase activity (Equation 14) the area asymmetry dynamics follow a monotonous increase (Fig. 7*C*). In this case the first equation of $\eta(t)$ describes the intercept of the curve $\eta(t)$ with $\eta = 0.001$, and the second equation accounts for the known maximal amount of lipid incorporation, which in this case (egg-LPC) has been already determined to be about 3% of total lipid (11).

Parameter values obtained from fitting the data of different experiments are presented in Table 1. The parameters $k_c b$ and k_m were determined by trial-fitting of the curve $\eta(t)$ (Equation 13) to the experimentally measured times t_1 and t_2. The fitting was performed by varying k_m and $k_c b$ at fixed values of parameters J and k_w (Equation 13). The values of J and k_w were determined from experiments on egg-LPC insertion into the outer monolayer of GUV in the absence of flippases and, hence, under conditions of negligible trans-monolayer lipid exchange. In this case the number of lipid molecules incorporated into the external monolayer related to the total number of the monolayer lipids, $\Delta N_{out}/N_{out}$, changes with time according to Equation 14. The coefficient for the resulting expression, Ja/k_w, represents the maximal possible value of $\Delta N_{out}/N_{out}$. Taking into account that for the concentrations used in our experiments the maximal value of $\Delta N_{out}/N_{out}$ is 0.03 (11), we obtain $Ja/k_w = 0.03$. Furthermore, experiments in the absence of flippases showed that bud formation corresponding to incorporation of 0.001 of total lipids (11, 12) occurred about 1 min after the addition of lipids to the solution (Fig. 2). Inserting this value together with $Ja/k_w \approx 0.03$ in the expression for $\Delta N_{out}/N_{out}$, we obtain $Ja = 0.001\ min^{-1}$, and $k_w = 0.03\ min^{-1}$.

All fitting procedures were only successful for values of k_m and $k_c b$ in a very narrow range, supporting the robustness of the fitting results. However, for some experiments fitting could not be achieved by using $Ja = 0.001\ min^{-1}$, and $k_w = 0.03\ min^{-1}$. In those cases the value for J was taken as a third fitting parameter.

Note that the dispersion range of the fitted values of $k_c b$ is rather large, with values differing by a factor of 10. This can be ascribed to the experimental setup in which the exact amount of membranes and, in particular, the total lipid concentration is not well controlled and may vary considerably between different experiments by the following reasons. Added lipids might stick to the glass bottom of the dish used for experiments, which

reduces the effective lipid concentration. The effective egg-LPC concentration on the vesicle membrane might also be influenced by uncontrolled kinetic restrictions since the egg-LPC solution was not stirred.

We estimated the sensitivity of the fitted values of k_m and $k_c b$ with respect to variation of J and k_w. Varying J and k_w within a range for which the experimental values of t_1 and t_2 could still be matched, the order of magnitude of the fitted parameters k_m and $k_c b$ did not change (see Table 2).

REFERENCES

1. Kornberg, R. D., and McConnell, H. M. (1971) *Biochemistry* **10,** 1111–1120
2. Holthuis, J. C. M., and Levine, T. P. (2005) *Nat. Rev. Mol. Cell Biol.* **6,** 209–220
3. Pohl, A., Devaux, P. F., and Herrmann, A. (2005) *Biochim. Biophys. Acta* **1733,** 29–52
4. Bishop, W. R., and Bell, R. M. (1985) *Cell* **42,** 51–60
5. Herrmann, A., Zachowski, A., and Devaux, P. F. (1990) *Biochemistry* **29,** 2023–2027
6. Buton, X., Morrot, G., Fellmann, P., and Seigneuret, M. (1996) *J. Biol. Chem.* **271,** 6651–6657
7. Marx, U., Lassmann, G., Holzhütter, H. G., Wüstner, D., Müller, P., Höhlig, A., Kubelt, J., and Herrmann, A. (2000) *Biophys. J.* **78,** 2628–2640
8. Hrafnsdóttir, S., Nichols, J. W., and Menon, A. K. (1997) *Biochemistry* **36,** 4969–4978
9. Devaux, P. F., Fellmann, P., and Hervé, P. (2002) *Chem. Phys. Lipids* **116,** 115–134
10. Mui, B. L., Döbereiner, H. G., Madden, T. D., and Cullis, P. R. (1995) *Biophys J.* **69,** 930–941
11. López-Montero, I., Rodriguez, N., Cribier, S., Pohl, A., Velez, M., and Devaux, P. F. (2005) *J. Biol. Chem.* **280,** 25811–25819
12. Berndl, K., Käs, J., Lipowsky, R., Sackmann, E., and Seifert, U. (1990) *Europhys. Lett.* **13,** 659–664
13. Farge, E., and Devaux, P. F. (1992) *Biophys. J.* **61,** 347–357
14. Tanaka, T., Sano, R., Yamashita, Y., and Yamazaki, M. (2004) *Langmuir* **20,** 9526–9534
15. Fellmann, P., Zachowski, A., and Devaux, P. F. (1994) *Methods Mol. Biol.* **27,** 161–175
16. Taxis, C., Hitt, R., Park, S. H., Deak, P. M., Kostova, Z., and Wolf, D. H. (2003) *J. Biol. Chem.* **278,** 35903–35913
17. Zinser, E., and Daum, G. (1995) *Yeast* **11,** 493–536
18. Angelova, M., Soleau, S., Meleard, P., Faucon, J. F., and Bothorel, P. (1992) *Prog. Colloid. Polym. Sci.* **89,** 127–131
19. Mathivet, L., Cribier, S., and Devaux, P. F. (1996) *Biophys. J.* **70,** 1112–1121
20. Girard, P., Pécréaux, J., Lenoir, G., Falson, P., Rigaud, J.-L., and Bassereau, P. (2004) *Biophys. J.* **87,** 419–429
21. Bligh, E. G., and Dyer, W. J. (1959) *Can. J. Med. Sci.* ***3*** **7,** 911–917
22. Rouser, G., Fleischer, S., and Yamamoto, A. (1970) *Lipids* **5,** 494–496
23. Leventis, R., and Silvius, J. R. (2001) *Biophys. J.* **81,** 2257–2267
24. John, K., Kubelt, J., Müller, P., Wüstner, D., and Herrmann, A. (2002) *Biophys. J.* **83,** 1525–1534
25. Hope, M. J., Redelmeier, T. E., Wong, K. F., Rodrigueza, W., and Cullis, P. R. (1989) *Biochemistry* **28,** 4181–4187
26. Nicolson, T., and Mayinger, P. (2000) *FEBS Lett.* **476,** 277–281
27. Kol, M. A., van Dalen, A., de Kroon, A. I., and de Kruijff, B. (2003) *J. Biol. Chem.* **278,** 24586–24593
28. Menon, A. K., Watkins, W. E., III, and Hrafnsdóttir, S. (2000) *Curr. Biol.* **10,** 241–252
29. De Kruyff, B., van den Besselaar, A. M., and van Deenen, L. L. (1977) *Biochim. Biophys. Acta* **465,** 443–453
30. Bhamidipati, S. P., and Hamilton, J. A. (1995) *Biochemistry* **34,** 5666–5677
31. Eckford, P. D. W., and Sharom, F. (2005) *Biochem. J.* **389,** 517–526
32. Kubelt, J., Menon, A. K., Müller, P., and Herrmann, A. (2002) *Biochemistry* **41,** 5605–5612
33. Kol, M. A., de Kroon, A. I., Killian, J. A., and de Kruijff, B. (2004) *Biochemistry* **16,** 2673–2681
34. Vishwakarma, R. A., Vehring, S., Mehta, A., Sinha, A., Pomorski, T., Herrmann, A., and Menon, A. K. (2005) *Org. Biomol. Chem.* **3,** 1275–1283
35. Quinn, P., Griffiths, G., and Warren, G. (1984) *J. Cell Biol.* **98,** 2142–2147
36. Alberty, R. A., and Silbey, R. J. (1983) *Physical Chemistry*, 6th Ed., pp. 275–296, John Wiley & Sons, Inc., New York
37. Adamson, A. W. (1990) *Physical Chemistry of Surfaces*, 3rd Ed., pp. 548–634, John Wiley & Sons, Inc., New York
38. Brown, S. D., Baker, B. L., and Bell, J. D. (1993) *Biochim. Biophys. Acta* **1168,** 13–22

Supplementary Information

Shape changes of GUVs correlate with transbilayer redistribution of exogenously added fluorescent lipids

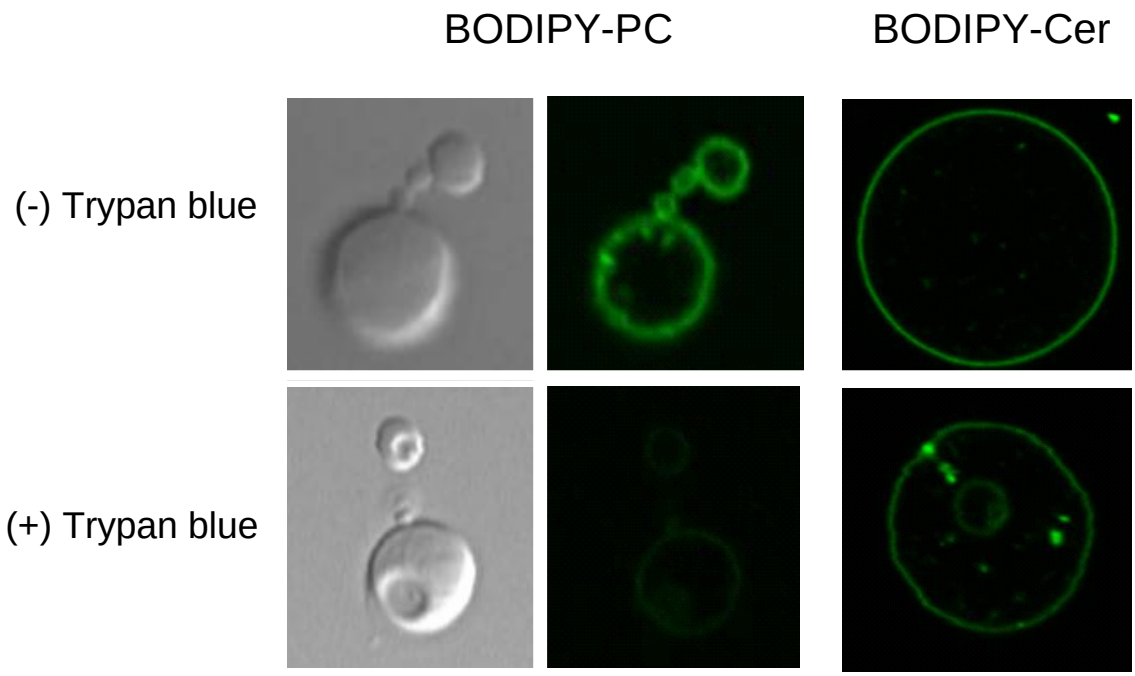

Supplementary Figure 1.
Transbilayer distribution of fluorescent lipids added exogenously to egg-PC GUVs. BODPIY-PC (left) and BODPIY-Cer (right) were added to egg-PC GUVs. After incubation for 30 min (BODIPY-PC) and 10 min (BODIPY-Cer), respectively, GUVs were imaged at room temperature on an Olympus FV1000 confocal microscope using a PlanSApo 60×/1.35 N.A. objective lens and a 488 nm laser. Fluorescence was recorded in the range from 500 nm to 530 nm before (top) or after (bottom) quenching the fluorescence of the surface-exposed BODIPY-lipids by the non-permeating quencher trypan blue (0.0075 % w/v). For BODIPY-PC, DIC images (left) are shown. Fluorescence of BODIPY-PC (top) was efficiently quenched upon addition of trypan blue (bottom). The pearl-chain like shapes of GUVs were observed only after longer incubation (~ 30 min) but not after shorter incubation (see Results). However, we selected those images to demonstrate that even after longer incubation BODIPY-PC could be efficiently quenched. In contrast, quenching of BODPIY-Cer was much less efficient under these conditions. Note, that images without or with trypan blue refer to different GUVs.

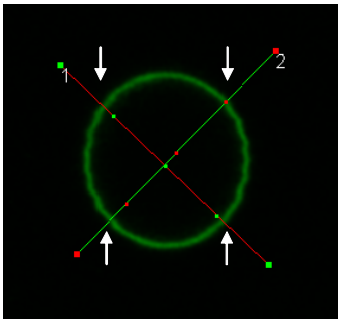

Supplementary Figure 2.
Analysis of surface-exposed BODIPY-lipid fraction in GUVs as employed for quantifying transbilayer lipid redistribution by trypan blue quenching. Fluorescence intensity of BODPIY-lipids incorporated into GUVs were taken from averaged confocal images through the equatorial plane. For each vesicle, the maximum intensity of four points (see arrows) was taken using Olympus FV10-ASW software.

GUVs containing CPM-labelled ER proteins

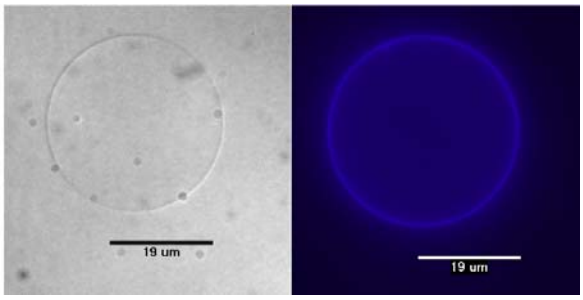

Supplementary Figure 3.

GUVs containing CPM-labelled ER proteins. Proteoliposomes reconstituted with covalently CPM labelled proteins of Triton extracts from microsomal yeast membranes were subsequently used for preparation of GUVs as described. GUVs were visualized by either DIC (left) or fluorescence (right). CPM: 7-diethylamino-3-(4'-maleimidylphenyl)-4-methylcoumarin.

Shape transition of GUVs prepared from proteoliposomes containing microsomal membrane proteins

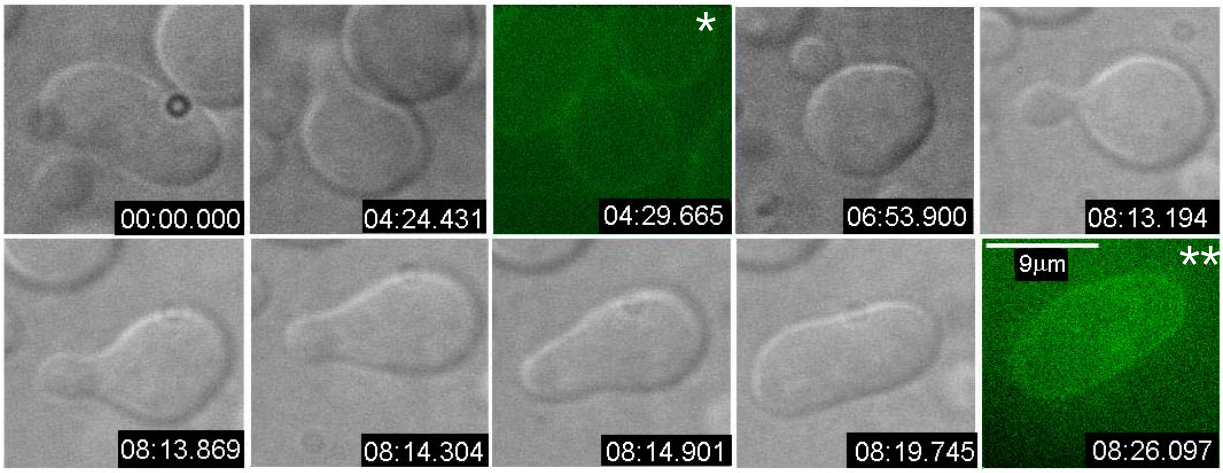

Supplementary Figure 4.
Shape transition of GUVs prepared from proteoliposomes containing microsomal membrane proteins (40,000 g fraction containing a GFP-tagged membrane protein). At time $t = 0$, egg-LPC was added. GUVs were visualized by either DIC or fluorescence microscopy at room temperature. The lipid/protein ratio was 35/1 (w/w). During the sequence fluorescence images were taken (* and **).